Isı Bilimi ve Tekniği Dergisi, 43, 2, 207-215, 2023
J. of Thermal Science and Technology
©2023 TIBTD Printed in Turkey
ISSN 1300-3615
e-ISSN 2667-7725
https://doi.org/10.47480/isibted.1391429

ANALYTICAL STUDY OF HEMISPHERICAL ICE SUBLIMATION IN ENCLOSURES WITH HUMIDITY AND FORCED CONVECTION

Mehmet Anil GULSAN*, Sedat TOKGOZ, Seyhan UYGUR ONBASIOGLU*****
*Department of Mechanical Engineering, Istanbul Technical University
34437 Gumussuyu, Istanbul, Turkey
anilgulsan@gmail.com, ORCID: 0000-0003-4667-6041
**Department of Aeronautical Engineering, Gebze Technical University
Istanbul, Turkey
sedattokgoz@gtu.edu.tr, ORCID: 0000-0002-0836-2861
***Department of Mechanical Engineering, Istanbul Technical University
34437 Gumussuyu, Istanbul, Turkey
onbasiogl1@itu.edu.tr, ORCID: 0000-0002-8386-2647

(Geliş Tarihi: 08.02.2022, Kabul Tarihi: 23.10.2023)

Abstract: In real life, sublimation of ice under certain conditions results in non-uniform formation of ice cubes with irregular shapes. During extracting these irregularly shaped cubes from enclosed spaces, the openings through which the cubes move can be plugged. A deep analysis of the sublimation process should be applied to make the shape of the ice cubes homogeneous and smooth-edged. Although there is an analytical method for the sublimation of spherical ice in literature, the hemispherical shape has not been studied. Furthermore, if ice formation and sublimation occur simultaneously within a place confined by a wall, novel approaches are necessary. In the current study, an analytical method has been proposed for the sublimation from a hemispherical ice sample as a combination of the models for the spherical and circular flat surfaces. The sublimation rate calculated by this new analytical method has been compared to the results from the weighing experiments and visualizations where the sublimation over time was measured by processing a series of images of ice cubes. There is a good agreement between the calculated values and the mass loss observed in the visualized images and the weighted samples. Thus, it is concluded that the sublimation rate is correlated with the velocity, temperature, and relative humidity of the air flowing over the ice cubes undergoing sublimation.
Keywords: Sublimation, visualization, transient mass transfer, ice

NEMLİ VE ZORLANMIŞ TAŞINIMLI KAPALI HACİMLERDE YARIKÜRESEL BUZ SÜBLİMASYONUNUN ANALİTİK İNCELENMESİ

Özet: Gerçek hayatta, buzun belirli koşullar altında süblimleşmesi, düzensiz şekilli buz küplerinin oluşumuyla sonuçlanır. Düzensiz şekilli bu küplerin kapalı alanlardan çıkarılması sırasında küplerin hareket ettiği açıklıklar tıkanabilir. Buz küplerinin şeklinin homojen ve düzgün kenarlı olması için süblimasyon prosesinin derinlemesine analizi gerçekleştirilmelidir. Literatürde küresel buzun süblimleşmesine yönelik analitik bir yöntem bulunmasına rağmen yarım küre şekli çalışılmamıştır. Ayrıca, duvarla sınırlandırılmış bir hacimde buz oluşumu ve süblimleşme aynı anda meydana geliyorsa, yeni yaklaşımlar gereklidir. Bu çalışmada, küresel ve dairesel düz yüzey modellerinin bir kombinasyonu olarak yarım küre şeklindeki bir buz örneğinden süblimleşme için analitik bir yöntem önerilmiştir. Bu yeni analitik yöntemle hesaplanan süblimleşme miktarı, süblimleşmenin bir dizi buz küpü görüntüsünün işlenmesiyle elde edildiği görselleştirme deneyleri ve tartım yapılarak elde edilen sonuçlarla karşılaştırıldı. Hesaplanan değerler ile görselleştirme sonuçlarında ve tartım yapılmış numunelerde gözlemlenen kütle kaybı arasında iyi bir uyum vardır. Elde edilen sonuçlara göre süblimleşme miktarının, süblimleşmeye uğrayan buz küplerinin üzerinden akan havanın hızı, sıcaklığı ve bağıl nemi ile ilişkili olduğu sonucuna varılmıştır.
Anahtar Kelimeler: Süblimleşme, görselleştirme, zamana bağlı kütle transferi, buz

NOMENCLATURE

A	equation coefficient [-]
A_s	surface area of circular flat surface [m^2]
B	equation coefficient [-]
D	diameter of sphere [m]

D_{AB} diffusion coefficient of water vapor (A) in air (B) [m^2/s]
g gravity [m/s^2]
Gr Grashof number for heat transfer [-]
Gr_m Grashof number for mass transfer [-]
h convection heat transfer coefficient [W/m^2K]
h_m convection mass transfer coefficient [m/s]
K equation coefficient [-]
k thermal conductivity of air [kW/mK]
L characteristic length [m]
L_s latent heat of sublimation [kJ/kg]
M molecular weight of water [kg/kmol]
m mass of water ice sample [kg]
n equation coefficient [-]
Nu_s Nusselt number of spherical surface [-]
Nu_f Nusselt number of circular flat surface [-]
P perimeter length of flat surface [m]
p equation coefficient [-]
P_s saturation pressure [kPa]
Pr Prandtl number [-]
r radius of sphere [m]
R_u universal gas constant [kJ/kmolK]
Ra Rayleigh number for heat transfer [-]
Ra_m Rayleigh number for mass transfer [-]
Re Reynolds number [-]
Sc_s Schmidt number of spherical surface [-]
Sc_f Schmidt number of circular flat surface [-]
Sh Sherwood number [-]
T absolute temperature [K]
T_∞ ambient temperature [K]
T_f film temperature [K]
T_r surface temperature of the sphere [K]
T_w wall temperature of the circular flat surface [K]

Greek Symbols
α equation coefficient [-]
β equation coefficient [-]
ν kinematic viscosity of air [m^2/s]
ρ average density of water vapor [kg/m^3]
ρ_∞ density of water vapor in the remote environment [kg/m^3]
ρ_r density of water vapor in the immediate vicinity of the sphere [kg/m^3]
ρ_s saturation density of vapor [kg/m^3]
ρ_w density of water vapor in the immediate vicinity of the circular flat surface [kg/m^3]
φ relative humidity [-]

INTRODUCTION

Not only for the snow analysis in meteorology, but also in novel refrigeration systems and cryogenics, sublimation is an important topic (Chen et al., 2014; Schmidt, 1972; Schmidt and Gluns, 1992). The findings in this area may be applied to the dissolution of solids, for instance for controlling the smoothness of surfaces during synthesis or for optimizing crystalline shapes during drug dissolution (Jambon-Puillet et al., 2018). As it is summarized in Zhao et al. (2020), theoretical studies on the sublimation process itself are rare, in contrary to being the fundamental phenomenon in de-icing and defrosting processes, food preservation, and porous media fabrication. In literature, investigations on naphthalene, solid carbon dioxide, benzoic acid (Aoki et al., 2002; Garner and Grafton, 1954; Hong and Song, 2007; Smolik and Vitovec, 1983), ice (Neumann et al., 2009; Schmidt, 1972; Schmidt and Gluns, 1992; Thorpe and Mason, 1966), and subcooled water droplets (Reitzle et al., 2019; Ruberto et al., 2017) are present. However, there is a lack of study on the sublimation during ice formation in domestic refrigerators.

In the current study, the sublimation rate of ice in an enclosed space under forced air flow conditions is visualized by an image processing method and also calculated from weighing experiments. Thus; the parameters of the sublimation rate are studied and a basic approach has been handled to understand the irregularities on the surfaces of the ice cubes resulting in plugging within the passages of the refrigerator. Since hemispherical ice samples are geometrically similar to the ice cubes formed in refrigerators, these shapes have been used as the domain geometry. As stated in Jambon-Puillet et al. (2018) sublimation from hemispherical shapes usually takes longer compared to other types of geometry and both weighing experiments and visualization processes depend on several parameters. Here, in addition to the ones reported in the literature, the temperature difference between the ice sample surface and the enclosure has been taken into account, as well as the humidity of the air within the enclosure. Moreover, the effect of the extreme temperature difference between the ice sample surface and enclosure on the sublimation rate is investigated with an analytical model for a variety of φ levels as a special case. Then the heat and mass transfer have been correlated to the velocity of the air over the ice samples, and the enclosure temperature. The results have been extended to predict ice plugging in a variety of conditions before it occurs and prevent it without any malfunctions.

ANALYTICAL METHOD FOR THE HEMISPHERE

Most of the analytical sublimation models study ice crystals, snow, and snowflakes in cold regions. They investigate sublimation rates on different geometries, especially on spherical and flat geometries. However, there is no sublimation model for the hemispherical geometry, presented in literature. A model developed for the sublimation of the spherical samples is not convenient with a hemispherical sample. In order to develop the model fully, the spherical and the flat surfaces should be investigated, separately.

In the present study, the model proposed for spherical bodies in literature Thorpe and Mason (1966) has been modified for the hemispherical geometry. By this modification, the model for the spherical surface of the hemisphere has been combined with the model for the flat surface. This modification has also considered that the circular flat surface of the hemisphere is not directly exposed to the freestream but it is located in the wake region facing the downstream (Figure 1).

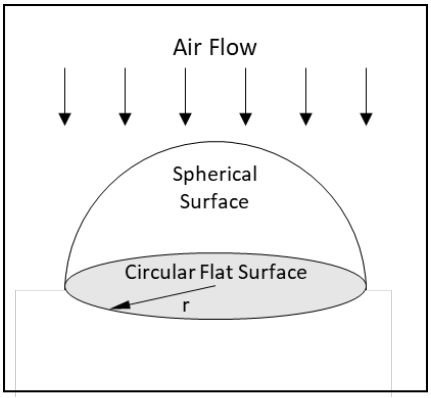

Figure 1. Hemispherical sublimation model.

The modified analytical model has been based on the spherical geometry studied by Thorpe and Mason (1966) where the temperature differences between the ice surface and environment were neglected. They used the diffusivity value (between water and air at 0°C) 7% lower than the reference value, which is 0.22 x 10^{-4} m^2/s.

However, in the current study, air temperature in the test section has an oscillation within ±3°C of the reference value. This difference is considered in the modification. On the other hand, the reference diffusivity value was taken as the same with Thorpe and Mason (1966) to keep the test-validated method as possible. The transient heat and mass transfer equations (Eq. 1 and Eq. 2) have been combined with the Clausius-Clapeyron equation (Eq. 3) as in Thorpe and Mason (1966). Finally, a model for the hemispherical surface (Eq. 12), also including temperature differences between the ice surface and the ambient, is formed. Then total sublimation rate was calculated, summing up the sublimation rate for the hemisphere and the circular flat surface (Eq. 23).

Equations for the sublimation rate in terms of heat transfer, and mass transfer given in Thorpe and Mason (1966) are as the followings

$$L_s \frac{dm}{dt} = 2\pi kr(T_r - T_\infty)Nu_s \tag{1}$$

$$\frac{dm}{dt} = 2\pi D_{AB} r(\rho_\infty - \rho_r)Sh_s \tag{2}$$

where Nu_s and Sh_s defined in Eq. (15a) and Eq. (15b).

On the other hand, the Clausius-Clapeyron equation with an ideal gas approximation is:

$$\frac{d\rho_s}{\rho_s} = \left(\frac{L_s M}{R_u T^2}\right) dT - \frac{dT}{T} \tag{3}$$

where boundary conditions are

$$T = T_\infty \rightarrow \rho_s = \rho_s(T_\infty) \tag{4}$$

$$T = T_r \rightarrow \rho_s = \rho_s(T_r) \tag{5}$$

Integrating Eq. (3) and applying boundary conditions (4 and 5) gives:

$$ln\left(\frac{\rho_s(T_r)}{\rho_s(T_\infty)}\frac{T_r}{T_\infty}\right) = \frac{L_s M}{R_u}\left(\frac{T_r - T_\infty}{T_\infty T_r}\right) \tag{6}$$

If water vapor density in the immediate vicinity of the ice surface is considered to be equal to the saturated vapor density at ambient temperature (i.e. $\rho_s = \rho_s(T_r)$), using Eq. (2)

$$\rho_r = \rho_s(T_r) = \rho_\infty - \frac{1}{2\pi D_{AB} r Sh_s}\frac{dm}{dt} \tag{7}$$

can be obtained.

Combining Eqs. (6) and (7) results in

$$ln\left[\left(\frac{\rho_\infty}{\rho_s(T_\infty)} - \frac{1}{2\pi D_{AB} r Sh_s \rho_s(T_\infty)}\frac{dm}{dt}\right)\frac{T_r}{T_\infty}\right] = \frac{L_s M}{R_u}\left(\frac{T_r - T_\infty}{T_\infty T_r}\right) \tag{8}$$

Here, $\rho_\infty/\rho_s(T_\infty)$ is equal to φ, at ambient temperature T_∞. Thus;

$$\left(\varphi - \frac{1}{2\pi D_{AB} r Sh_s \rho_s(T_\infty)}\frac{dm}{dt}\right)\frac{T_r}{T_\infty} = e^{\frac{L_s M}{R_u}\left(\frac{T_r - T_\infty}{T_\infty T_r}\right)} \tag{9}$$

is obtained.

If a series expansion is performed for the right-hand side of the above equation:

$$\left(\varphi - \frac{1}{2\pi D_{AB} r Sh_s \rho_s(T_\infty)}\frac{dm}{dt}\right)\frac{T_r}{T_\infty} = 1 + \frac{L_s M}{R_u}\left(\frac{T_r - T_\infty}{T_\infty T_r}\right) + \frac{1}{2}\left(\frac{L_s M}{R_u}\right)^2\left(\frac{T_r - T_\infty}{T_\infty T_r}\right)^2 + \cdots \tag{10}$$

Since the third and the following terms can be considered as a truncation error because of their relatively small values,

$$\left(\varphi - \frac{1}{2\pi D_{AB} r Sh_s \rho_s(T_\infty)}\frac{dm}{dt}\right)\frac{T_r}{T_\infty} = 1 + \frac{L_s M}{R_u}\left(\frac{T_r - T_\infty}{T_\infty T_r}\right) \tag{11}$$

is obtained.

Combining Eq. (1) and Eq. (11) and rearranging and dividing by 2, the sublimation rate for the hemispherical surface can be calculated:

$$\frac{dm}{dt} = \frac{\pi r\left(\varphi - \frac{T_\infty}{T_r}\right)}{\left(\frac{1}{D_{AB} Sh_s \rho_s (T_\infty)}\right) + \left(\frac{{L_s}^2 M}{R_u k Nu_s {T_r}^2}\right)} \qquad (12)$$

Nu_s and Sh_s appearing in Eq. (12) have been calculated by substituting the experimental mass change into Equations (1) and (2). Mass transfer due to natural convection from the lower surface of the hemisphere has been calculated from the relevant correlations and subtracted from the total mass measured during the experiments. Sherwood numbers from the experimental data for the hemisphere under study have been compared to the correlations reported in the literature (Figure 2).

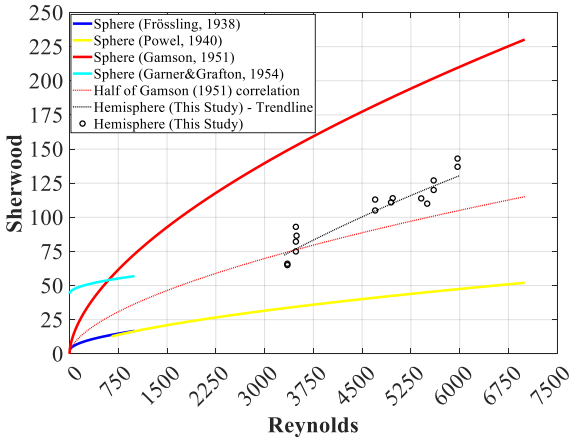

Figure 2. Comparison of the Sherwood correlation for the hemisphere with the Sh correlations for the sphere in the literature.

It is seen that Sherwood numbers from the current experimental results coincide with the half of the correlation for spherical surfaces by Gamson (1951). The maximum variation is 24.2% at Reynolds 6000 between the trendline of experimental results and the half of the Gamson (1951) correlation.

On the other hand; the wind factor curve was generated using weighing results as in previous studies (Pasternak and Gauvin, 1960; Pitter et al., 1974; Thorpe and Mason, 1966). For spherical bodies, the correlations below have been used:

$$Nu_s = B + \beta Re^n Pr^p \qquad (13)$$

$$Sh_s = A + \alpha Re^n Sc^p \qquad (14)$$

where Reynolds number is based on the diameter (Garner and Grafton, 1954; Pitter et al., 1974; Thorpe and Mason, 1966).

For the coefficients appearing in correlations, there are different values in the literature. For the quiescent environment (Re = 0), A = B = 2 is proposed by Langmuir (1918) and validated by Frossling (1938) and Ranz and Marshall (1952). For low Reynolds number cases (10<Re < 200), A = B = 1.88 is obtained by Thorpe and Mason (1966).

In the presented study, the range is as 3300<Re<6000. Thus, the wind factor, F values in Pasternak and Gauvin (1960), Pitter et al. (1974), Thorpe and Mason (1966) have been used to determine A, B, α, and β coefficients of Nu_s and Sh_s correlations.

In Powell (1940) for 650≤Re≤45000, also in Pasternak and Gauvin (1960) for 500 < Re < 5000, and in Gamson (1951) without regarding to the Reynolds number, it is given as p=1/3 and n=0.5. Considering p and n independent of geometric shapes, and the moderate range of the Reynolds numbers in the current study, p=1/3 and n=0.5 are assumed. Thus, the following equations in terms of wind factor are obtained (Figure 3).

$$Nu_s = 3.432 Re^{1/2} Pr^{1/3} - 94.942$$
3300<Re<6000 (15a)

$$Sh_s = 3.432 Re^{1/2} Sc^{1/3} - 94.942$$
3300<Re<6000 (15b)

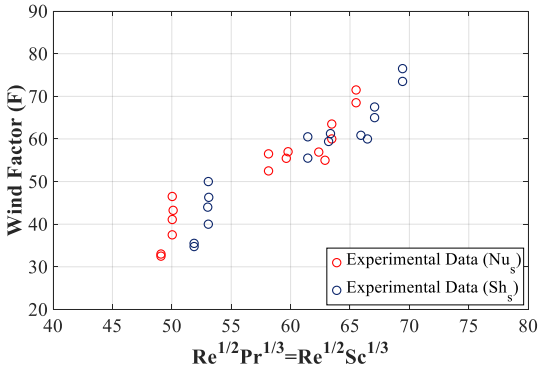

Figure 3. Investigation of heat and mass transfer correlations as a single equation by using wind factor.

Eq. (15b) is identical to the correlation $Sh=0.85Re^{0.59}Sc^{0.33}$ which is validated by the experimental data illustrated in Figure 2. The discrepancy between the resulted correlation, and the one obtained as the half of Gamson's has emerged due to the uncertainty of the experiments. The natural convection from the flat surface of the hemisphere may be another reason for this difference.

The sublimation rate from the flat surface can be written in terms of the Nusselt number, and Sherwood number (Goldstein et al.,1973; Incropera, 2011; Lloyd and Moran, 1974):

$$L_s \frac{dm}{dt} = (T_w - T_\infty) \frac{4 Nu_f k}{D} \frac{\pi . D^2}{4} = 2\pi r k Nu_f (T_w - T_\infty)$$

(16)

$$\frac{dm}{dt} = (\rho_\infty - \rho_w)\frac{4Sh_f D_{AB}}{D}\frac{\pi . D^2}{4} = 2\pi r D_{AB} Sh_f (\rho_\infty - \rho_w)$$

(17)

With Clausius Clapeyron equation (Eq. 3) and ideal gas equation of state, the sublimation rate from the circular flat surface (Figure 1) is obtained as:

$$\frac{dm}{dt} = \frac{2\pi r\left(\varphi - \frac{T_\infty}{T_w}\right)}{\left(\frac{1}{D_{AB} Sh_f \rho_S(T_\infty)}\right) + \left(\frac{{L_S}^2 M}{R_u k Nu_f {T_w}^2}\right)} \quad (18)$$

For the flat surface, natural convection correlations (Goldstein et al., 1973; Incropera, 2011; Lloyd and Moran, 1974) have been used:

$$Nu_f = 0{,}54 Ra^{1/4} \quad (19)$$

$$\mathrm{Sh}_f = 0{,}54 Ra_m^{1/4} \quad (20)$$

As the characteristic length, L, is equal to r/2 for the circular surface; heat and mass transfer Rayleigh numbers appearing in the equations are:

$$\mathrm{Ra} = \mathrm{Gr} Pr = \frac{g\beta|T_S - T_\infty|}{\nu^2}\frac{D^3}{64} Pr \quad (21)$$

$$Ra_m = Gr_m Sc = \frac{g(\rho_S - \rho_\infty)}{\rho \nu^2}\frac{D^3}{64} Sc \quad (22)$$

Finally, the total sublimation rate of hemispherical ice is defined as:

$$\frac{dm}{dt} = \frac{\pi r\left(\varphi - \frac{T_\infty}{T_r}\right)}{\left(\frac{1}{D_{AB} Sh_S \rho_S(T_\infty)}\right) + \left(\frac{{L_S}^2 M}{R_u k Nu_S {T_r}^2}\right)} + \frac{2\pi r\left(\varphi - \frac{T_\infty}{T_w}\right)}{\left(\frac{1}{D_{AB} Sh_f \rho_S(T_\infty)}\right) + \left(\frac{{L_S}^2 M}{R_u k Nu_f {T_w}^2}\right)} \quad (23)$$

where the first term represents the spherical surface of the hemisphere and the second term corresponds to the sublimation rate from the bottom flat surface.

Here, the effects of the flow separations and vortices at the wake of the hemisphere and acting on the flat bottom surface have been neglected.

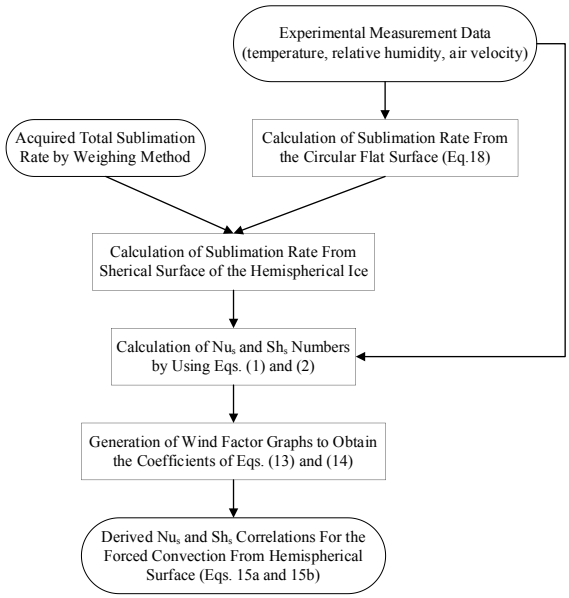

Figure 4. Flow chart for Nu_s and Sh_s correlations.

Once the required correlations were formed (Figure 4), Eq. (23) was analytically solved with a time step of 60 seconds which is the data sampling interval of the experiments. Since, it was confirmed by the recorded images of the ice sample (see the next section) that the ice shape changed homogeneously, throughout the spherical surface, the numerical procedure has not considered a varied sublimation rate.

EXPERIMENTAL SETUP

For the test rig, a wind tunnel has been installed on the refrigerator shelf within a well-insulated cabinet. The wind tunnel directs the air to flow over the hemispherical ice cube. As illustrated in Figure 5; the tunnel consists of an axial fan (A), flow straightener (B), and ice sample (C). The dimensions of the air tunnel are 90 mm x 90 mm x 300 mm. To enable optical access, tunnel walls were made up of transparent plexiglass. K-type thermocouples (T) and MSI HTG3500 relative humidity sensors (H) have been used to collect data from experiments with a data acquisition system. The thermocouples have been placed onto the tunnel entry and immediate vicinity of the flat surface of the ice sample. The flat surface temperature values have been used as identical to those of the spherical surface. In other words, the temperature distribution whole over the surfaces has been assumed as uniform. Also, φ data from the refrigerator ambient and inside of the tunnel has been measured. Both temperature and humidity data have been recorded with a sampling rate of 0.017 Hz (recording every 60 seconds). The velocity inside the tunnel has been controlled by changing the rotational speed of the DC-controlled fan.

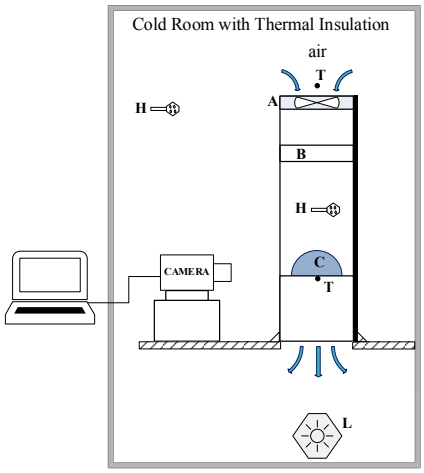

Figure 5. The experimental setup. A: Axial fan B: Flow straightener C: Ice sample H: Humidity sensors L: LED T: Thermocouples

Visualizations of the ice cubes were performed using a USB-controlled RGB camera with 15 megapixels resolution was placed at a 100 mm distance from the tunnel wall, for the image acquisition. Except for the observation window facing the camera, the walls of the tunnel were painted black in order to increase the contrast between the ice and the background of the images. A LED light (L) was used for illumination. NI Vision Builder ® software was used to periodically (1 image per hour) record the images of the hemispherical ice. An image processing algorithm in MATLAB® was developed to analyze the recorded images. The algorithm was used to determine the number of pixels forming the ice for each image and to detect the difference between successive images. Using this approach, it is possible to determine the change in the shape and the volume of the ice cube over time. In Figure 6, the purple field in the comparison image represents the change in the ice sample due to the sublimation. These results are compared to the results of weighing measurements that are discussed below.

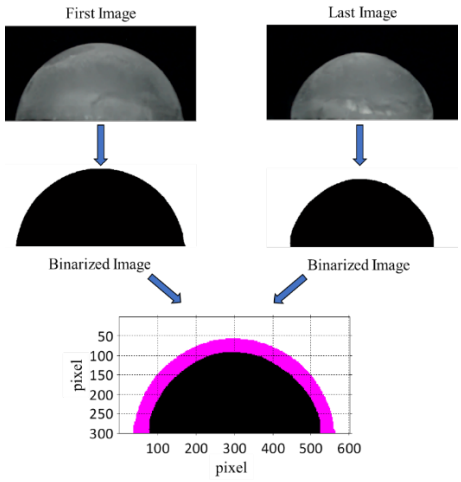

Figure 6. An example of the process of visualization for the -18°C forced convection with 1m/s air velocity case. The left image is recorded at the start of the measurements, while the image on the right is recorded after 72 hours. The difference in the projection of the two ice cubes is indicated by purple at the bottom graph.

The average air velocity in the test section has been measured by using particle image velocimetry (PIV). A HiSense Mk II camera with a resolution of 1344 x 1024 pixels was used for recording the PIV images. The light source for illumination was a double-pulsed Nd:YAG laser (New Wave Solo-III) with 50 mJ/pulse energy at a wavelength of 532 nm. The flow was seeded with paraffin oil smoke with a mean diameter of 1.5 µm. The vector fields were calculated using an interrogation window size of 32×32pixels and 50% of overlap. An average of 100 instantaneous vector fields were used to compute the average air velocity in the test section.

Mass loss due to sublimation was detected by also weighing the ice samples with KERN DE35K0.5D digital scale having a resolution value of ±0.5 g. Weighing measurements were performed at room temperature, rapidly so as not to allow additional sublimation or melting, after taking out the ice samples from the controlled (cold) room. At the beginning of each experiment, ice samples were weighted to check the initial mass of each sample. Also, they were weighted at the end of each experiment, and sublimated mass was calculated from the difference between two consecutive weighing measurements. The weighing was not continuous throughout the measurement duration. Thus, the results of the weighing measurements include only the initial and the final mass for each sample. Residual mass is calculated from the difference between these two values at the end of the weighting process. Each experiment was repeated twice to avoid possible errors and provide consistency between the image results.

CASE CONDITIONS AND MEASUREMENTS

In addition to the parameters such as temperature, air velocity, size of ice particles, and geometrical shape used in previous studies (Neumann et al., 2009; Thorpe and Mason, 1966), also ice storage time in the refrigerator is investigated. Since the purpose is to prevent the plugging within the ice-extracting channels, duration is an important parameter.

The hemispherical ice samples that were used in this study are 50 grams each and have 30 mm of radius. The ice sublimation rates were studied at two different ambient temperatures (-18°C and -24°C), which are the set temperatures of the refrigerator. To adjust the airspeed, 3 different voltage values of the axial fan were used, which are 6V, 9V, and 12V corresponding to 0.7m/s, 1m/s, and 1.2m/s. The experiments were carried out at two different durations, 72 and 144 hours. Although the value is between 50% and 70% for the refrigerators, the φ in the cold room could not be kept constant as also stated in Reitzle et al. (2019). Thus, φ was not able to be used as a controlled parameter for the experiments, but it was acquired for using in the analytical calculations (Eq. 23).

Residual mass which is the ratio of the remaining ice mass to the initial ice mass has been calculated from the weighing measurements and observed during the visualizations. Then, this ratio has been compared to the one calculated by the analytical method (Eq. 23). It is seen that the differences between the calculations, visualizations, and analytical method developed in the current are lower than 8% (Figure 7).

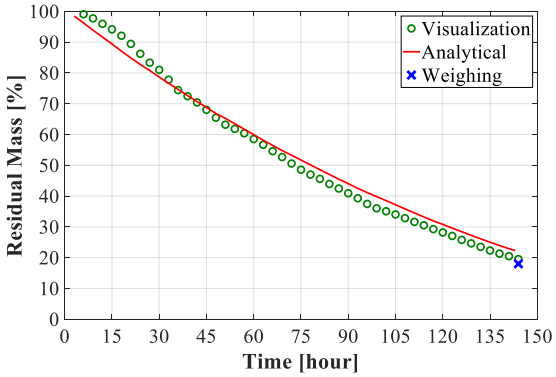

Figure 7. Ice sublimation results for -18 °C temperature; 1.2 m/s air velocity and 144 hours.

RESULTS

The effects of different parameters on the sublimation rate of hemispherical ice (Figure 8) have been measured and observed. Although the volumes of the ice cubes reduced significantly over time, the geometries mainly remained hemispherical during the sublimation process (see Figure 6). This is further confirmed by the samples weighed at the end of each experimental campaign, where the shapes of the ice cubes were axially symmetric. This shows that the sublimation of the hemispherical ice cubes occurs homogeneously over the hemispherical surface in our experimental setup, probably due to the shape of the test rig.

The sublimation rate depends on ambient temperature and air velocity. An increase in the ambient temperature at a constant air velocity results in a higher sublimation rate. On the other hand, the almost linear characteristics of the curves in Figure 8 show that the sublimation rate does not change with time. The sublimation rate is directly proportional to the air velocity at a constant ambient temperature.

According to the experimental results; in order to decrease the ice sublimation rate, the φ in the environment should be high and the temperature of the environment and air velocity values should be low.

Error analysis of experimental measurements has been given in Figure 9. Errors between the weighing and analytical study are lower than 6%. That shows the good correlation of these two methods. The errors of visualization are relatively higher compared to the other two methods, but all of the errors are lower than 10%. Also, it should be noted that the visualization method can be developed to give more accurate results with better a camera and equipment.

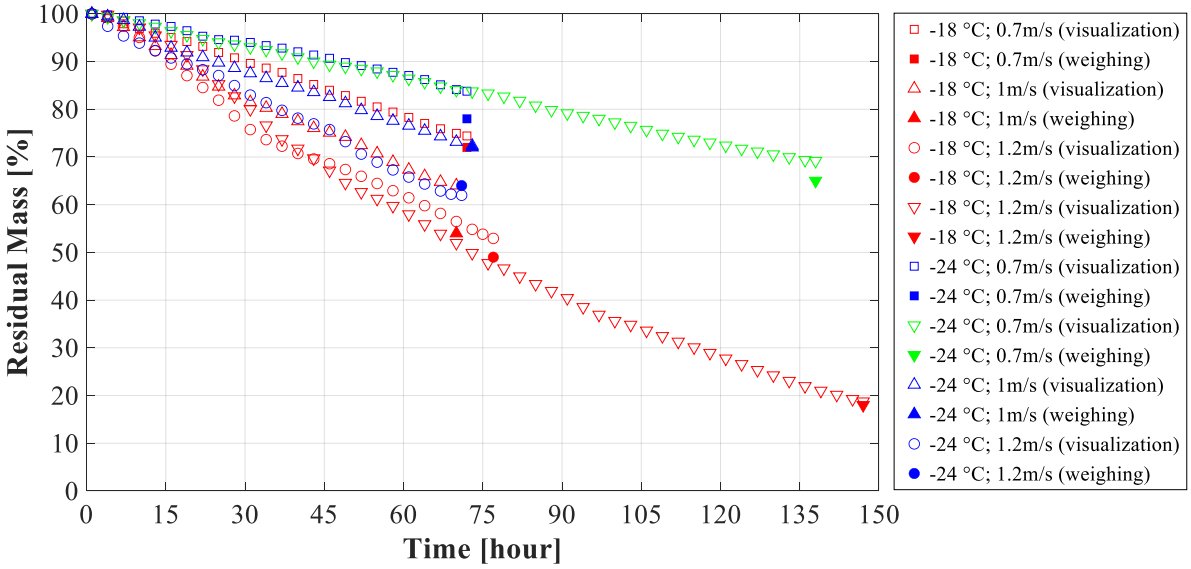

Figure 8. Change of the measured and observed residual mass with respect to time.

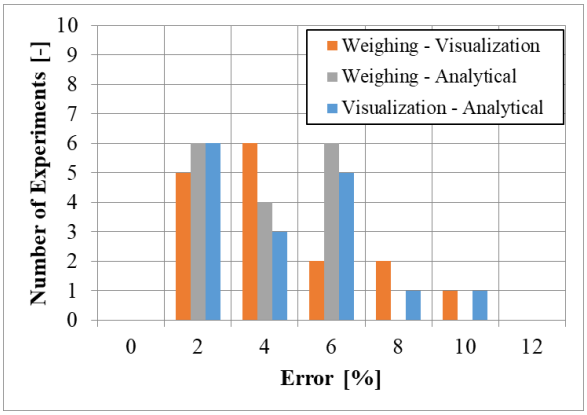

Figure 9. Error analysis of experimental measurements and analytical calculations

The theoretical sublimation amount of the hemispherical ice sample calculated using the analytical sublimation model (initially 50 grams) within one day are given in Figure 10, Figure 11, and Figure 12 for different temperature differences, relative humidities, and air velocities. The "residual mass rate" shows the residual mass of ice as a daily percentage by referencing the initial mass. As the φ decreases, residual mass changes parabolically with respect to the temperature in Figure 10. Also, if the surface temperature and the ambient temperature are identical, obviously there will be no sublimation or solidification if the air is saturated.

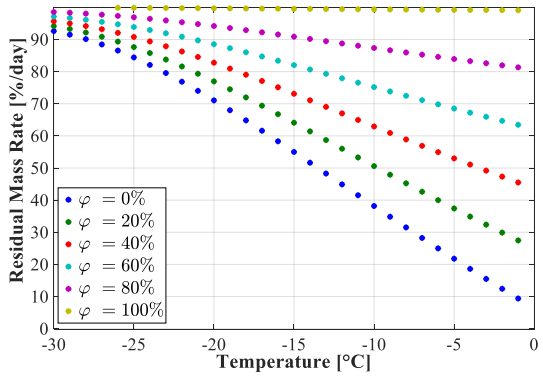

Figure 10. Residual mass rates at different temperatures and φ values for air velocity 1 m/s, and $T_r = T_w = T_\infty$ - 3 °C).

Analytical results of the sublimation model with relatively high-temperature differences between the ice sample and ambient are given in Figure 11 as a specific case. It is seen that φ values are less effective than the ones at 3 °C temperature difference illustrated in Figure 10.

In Figure 12, the residual mass rate for different air velocities is illustrated. The sublimation rate increases as the air velocity increases at a constant temperature. However, the amount of increment depends on temperature. For example, a residual mass difference between 0.6 m/s and 0.8 m/s air velocities is 6.2% at -10°C, while it is 2.74% at -20°C. Also, it is seen that the amount of increment is inversely proportional to the airspeed. The residual mass difference decreases from 6.2% (between 0.6 m/s and 0.8 m/s) to 4.22% (between 1.4 m/s and 1.6 m/s), as the velocity increases at -10°C.

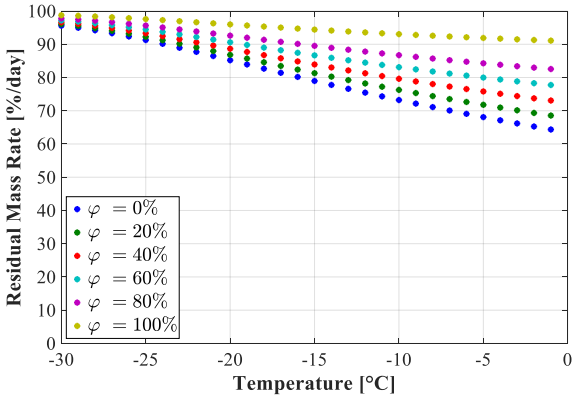

Figure 11. Residual mass rates at different temperatures and φ values for air velocity 1 m/s, $T_r = T_w = T_\infty$ - 100°C.

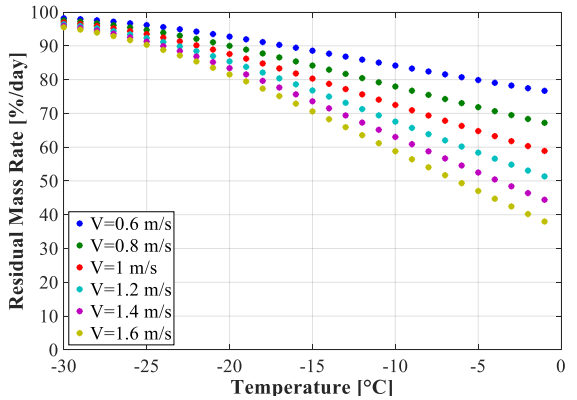

Figure 12. Residual mass rates at different temperatures and air velocity values in forced convection (φ =50% in the environment, $T_r = T_w = T_\infty$).

CONCLUSION

A new transient analytical model for the sublimation from a hemispherical ice sample is proposed as a combination of the models for the spherical and circular flat surfaces in this paper. The novel analytical method has been compared to two separate experimental methods, under forced convection conditions. Image processing-based visualization and weighing methods were carried out simultaneously to observe the sublimation phenomena. Experiments were performed at various temperatures, as well as different air velocities corresponding to 3300 < Re < 6000. The results of the analytical method are in good agreement with the calculated residual ice mass, via visualization and the weighted samples. The analytical model was employed to predict ice plugging depending on the sublimation rate of the ice sample under various conditions and to prevent it without undesired formations. Such an analytical method will be used to understand the irregularities on the surfaces of the hemispherical ice cubes, resulting from the parameters affecting the sublimation rate.

ACKNOWLEDGEMENT

The experimental activities of this work were conducted in the R&D laboratory of Arcelik Co. by the first and second authors.

REFERENCES

Aoki, K., Sawada, M., & Akahori, M. (2002). Freezing due to direct contact heat transfer including sublimation. *Int. Journal of Refrigeration*, *25*(2), 235–242. https://doi.org/10.1016/s0140-7007(01)00084-6

Chen, L., & Zhang, X.-R. (2014). A review study of solid–gas sublimation flow for refrigeration: From basic mechanism to applications. *Int. J. of Ref.*, *40*, 61–83. https://doi.org/10.1016/j.ijrefrig.2013.11.015

Frossling, N. (1938). Uber die Verdunstung fallender Tropfen. *Gerlands Beitrage Geophysik*, 52:170–216.

Gamson, B.W. (1951). Heat and mass transfer fluid solid systems. *Chem. Eng. Prog. 47* (1): 19-28

Garner, F. H., & Grafton, R. W. (1954). Mass transfer in fluid flow from a solid sphere. *Proceedings of the Royal Society of London. Series A. Mathematical and Physical Sciences*, *224*(1156), 64–82. https://doi.org/10.1098/rspa.1954.0141

Goldstein, R. J., Sparrow, E. M., & Jones, D. C. (1973). Natural convection mass transfer adjacent to horizontal plates. *Int. J. of Heat and Mass Transfer*, *16*(5), 1025–1035. https://doi.org/10.1016/0017-9310(73)90041-0

Hong, K., & Song, T.-H. (2007). Development of optical naphthalene sublimation method. *Int. J. of Heat and Mass Transfer*, *50*(19-20), 3890–3898. https://doi.org/10.1016/j.ijheatmasstransfer.2007.02.017

Incropera, F. P. (2011). *Fundamentals of heat and mass transfer* (7th ed.). John Wiley.

Jambon-Puillet, E., Shahidzadeh, N., & Bonn, D. (2018). Singular sublimation of ice and snow crystals. *Nature Com.*, *9* (1). https://doi.org/10.1038/s41467-018-06689-x

Langmuir, I. (1918). The Evaporation of Small Spheres. *Physical Review*, *12*(5), 368–370. https://doi.org/10.1103/physrev.12.368

Lloyd, J. R., & Moran, W. R. (1974). Natural Convection Adjacent to Horizontal Surface of Various Planforms. *Journal of Heat Transfer*, *96*(4), 443–447. https://doi.org/10.1115/1.3450224

Neumann, T. A., Albert, M. R., Engel, C., Courville, Z., & Perron, F. (2009). Sublimation rate and the mass-transfer coefficient for snow sublimation. *Int. J. of Heat and Mass Transfer*, *52*(1-2), 309–315. https://doi.org/10.1016/j.ijheatmasstransfer.2008.06.003

Pasternak, I. S., & Gauvin, W. H. (1960). Turbulent heat and mass transfer from stationary particles. *The Canadian Journal of Chemical Engineering*, *38*(2), 35–42. https://doi.org/10.1002/cjce.5450380202

Pitter, R. L., Pruppacher, H. R., & Hamielec, A. E. (1974). A Numerical Study of the Effect of Forced Convection on Mass Transport from a Thin Oblate Spheroid of Ice in Air. *J. of the Atmospheric Sciences*, *31*(4), 1058–1066. https://doi.org/10.1175/1520-0469(1974)031<1058:ansote>2.0.co;2

Powell, R.W. (1940). Further experiments on the evaporation of water from saturated surfaces. *Trans. Inst. Chem. Eng.* 18: 36

Ranz, W. and Marshall, W. (1952). Evaporation from drops. *Chem. Engineering Progress,* 48 (3): 141-146.

Reitzle, M., Ruberto, S., Stierle, R., Gross, J., Janzen, T., Weigand, B. (2019). Direct numerical simulation of sublimating ice particles. *Int. J. of Thermal Sciences*, 145, 105953. https://doi.org/10.1016/j.ijthermalsci.2019.05.009

Ruberto, S., Reutzsch, J., Roth, N., & Weigand, B. (2017). A systematic experimental study on the evaporation rate of supercooled water droplets at subzero temperatures and varying relative humidity. *Experiments in Fluids*, 58(5). https://doi.org/10.1007/s00348-017-2339-5

Schmidt R. and Gluns D. (1992). Sublimation of snow--the basics. *Proceedings, International Snow Science Workshop, Breckenridge, Colorado, USA* pp. 11-17

Schmidt R. A. (1972). Sublimation of wind-transported snow: a model. *U.S. Dept. of Agriculture, Forest Service, Rocky Mountain Forest and Range Experiment Station.*

Smolík, J., & Vítovec, J. (1983). Transient heat and mass transfer in the two-phase system: Subliming solid-vapour-gas mixture. *Int. J. of Heat and Mass Transfer*, 26(7), 975–980. https://doi.org/10.1016/s0017-9310(83)80122-7

Thorpe, A. D., & Mason, B. J. (1966). The evaporation of ice spheres and ice crystals. *British Journal of Applied Physics*, 17(4), 541–548. https://doi.org/10.1088/0508-3443/17/4/316

Zhao, Y., Guo, Q., Lin, T., & Cheng, P. (2020). A review of recent literature on icing phenomena: Transport mechanisms, their modulations and controls. *Int. J. of Heat and Mass Transfer*, 159, 120074. https://doi.org/10.1016/j.ijheatmasstransfer.2020.120074